Scientific Papers. Series E. Land Reclamation, Earth Observation & Surveying, Environmental Engineering. Vol. XIV, 2025
Print ISSN 2285-6064, CD-ROM ISSN 2285-6072, Online ISSN 2393-5138, ISSN-L 2285-6064

HYBRID MODELLING APPROACHES FOR LAND USE/LAND COVER CHANGE PREDICTION AND CARBON DYNAMICS IN MAROWIJNE, SURINAME

Tamara MYSLYVA[1, 2], Christiaan Max HUISDEN[2], Marek MROZ[3], Nataliia TSUMAN[4], Yurii BILYAVSKYI[4]

[1]Ministry of Spatial Planning and Environment of Suriname,
22 Prins Hendrikstraat, Paramaribo, Republic of Suriname
[2]Anton de Kom University of Suriname, 86 Leysweg, Paramaribo, Republic of Suriname
[3]University of Warmia and Mazury in Olsztyn,
Michała Oczapowskiego, 1 Street, 10-719, Olsztyn, Poland
[4]Zhytomyr Agricultural Technical Professional College,
96 Pokrovska Street, 10008, Zhytomyr, Ukraine

Corresponding author email: byrty41@yahoo.com

Abstract

Land use changes monitoring and predicting, as well as assessing their impact on carbon storage dynamics, play a pivotal role in addressing environmental challenges and ensuring effective land use management. This study aims to identify land use changes and their impact on carbon storage in the Marowijne district of Suriname from 2017 to 2024 and predict changes for 2034. Sentinel-2 images were used to analyze land change patterns and predict future trends. A hybrid approach combining Markov chain analysis, cellular automata, multilayer perceptron, support vector machines, and logistic regression was used to forecast future land use dynamics, while InVEST and YASSO models were utilized for carbon storage and sequestration predictions. The support vector machine-Markov chain hybrid model achieved an impressive accuracy of over 97%, outperforming other hybrid models. This model is recommended for generating land use change prediction maps, providing a crucial baseline for sustainable land use management. During the subsequent decade (2024-2034), the net loss of high-carbon areas is expected to intensify, affecting 15-20% of the district's territory. The identified spatiotemporal distribution of carbon storage provides valuable insights that will play a key role in achieving the objectives of Suriname's national green development strategy.

Key words: *land cover change dynamics, hybrid prediction models, carbon storage dynamics.*

INTRODUCTION

With significant impact on ecosystems and human lives, land use change is one of the major forces behind environmental and socioeconomic transformations. Analysing spatiotemporal patterns of land use and land cover (LULC) changes provides essential insights for sustainable land management and environmental conservation (van Ommeren-Myslyva et al., 2024; Devi & Shimrah, 2023; Girma et al., 2022). Understanding and managing land assets, natural resources, and environmental dynamics requires creating reliable LULC change predictive models (Song et al., 2020; Kafy et al., 2021). By providing valuable data on land potential and degradation risks, these models offer relevant and useful information on land suitability for various types of use or exploitation (Lambin & Meyfroidt, 2019; Aloqaili et al., 2021). Additionally, LULC modelling contributes to climate change mitigation by improving our understanding of carbon sequestration potential across different land cover types (Deng et al., 2020; Luo et al., 2021). Predicting land use change requires advanced methodologies that analyze historical data and observed trends to project future land cover patterns (van Ommeren-Myslyva et al., 2024). Several modelling approaches are commonly used, including statistical methods (Yeh & Liaw, 2021), Cellular Automata (CA) models (Muhammad et al., 2021), Markov Chain (MC) models (Mohamed & Worku, 2020), hybrid models (Asif et al., 2023), and multi-agent-based models (Robinson et al., 2021). Among these, hybrid models, which combine multiple predictive techniques to

leverage their respective strengths, have shown greater accuracy in forecasting future LULC changes. Suriname's forest ecosystems play a crucial role in global carbon dynamics, acting both as a major carbon reservoir and a significant net carbon sink. Between 2001 and 2023, these forests sequestered approximately 28.3 $MtCO_2e$ per year while emitting an average of 8.38 $MtCO_2e$ annually, resulting in a net carbon sink of -19.9 $MtCO_2e$ per year (Global Forest Watch, 2024). Land use and land cover are fundamental to carbon regulation, as changes in LULC deeply affect the capacity of ecosystems to store and sequester carbon (Sarathchandra et al., 2021). Suriname's ranking among the top three countries for High Forest Cover and Low Deforestation (HFLD) underscores its pivotal role in mitigating climate change. However, the ability of its forest ecosystems to store and sequester carbon is at risk due to changes in forest cover, whether from land conversion, land consumption, deforestation, or other land use and land cover alterations. To understand how these changes affect carbon storage, it is essential to evaluate carbon dynamics and predict the potential impacts on carbon budgets. This information is essential for creating land management plans that safeguard Suriname's forests and strengthen their ability to combat climate change. Marowijne – a district in Suriname – is facing increasing pressure on its land due to factors like urban growth, infrastructure development, and natural challenges such as a changing coastline and the impacts of climate change. To ensure the region's long-term sustainability and protect its natural environment, it's crucial to better understand these ongoing changes. Despite the clear occurrence of land use changes in Marowijne, there is a significant gap in studies that focus on detecting current trends, predicting future land use and land cover dynamics, and assessing the impact of land use changes on carbon storage and sequestration.

This study aims to achieve four interconnected objectives: (1) to collect and process geospatial data on land use and land cover; (2) to evaluate the accuracy and reliability of hybrid predictive models combining Markov chains with cellular automata (CA), multilayer perceptron (MLP), support vector machines (SVM), and logistic regression (LR) in predicting future land use changes within the Marowijne district of Suriname; (3) to develop a robust hybrid simulation model for forecasting LULC changes over the next 10 years; and (4) to project the spatial distribution of carbon storage and sequestration.

MATERIALS AND METHODS

Study area

The area of interest is Marowijne, a district of Suriname covering a total area of 4803 km^2, situated in the north-eastern part of the country. Geographically, Marowijne is located to the north between 4.0° and 5.95° N and to the west between 54.0° and 54.80° W mostly within the Young and Old Coastal Plains (only the southern and south-eastern parts are situated within the Savanna Belt and Interior Uplands), ranging from 35 below to 572 m above MSL. The district is divided into six administrative units (resorts), namely Galibi, Moengo, Moengo Tapoe, Wanhatti, Albina and Patamacca.

Figure 1 depicts the research area's location. The climate of the study area is tropical-equatorial (Af) according to the Köppen-Geiger climate classification. The soil cover is represented by Umbric Gleysols, Albic Plinthosols and Albic Arenosols according to the international soil classification system (WRB, 2014).

Datasets used. This study used three satellite image sets to analyze LULC change dynamics and build a predictive model (Table 1).

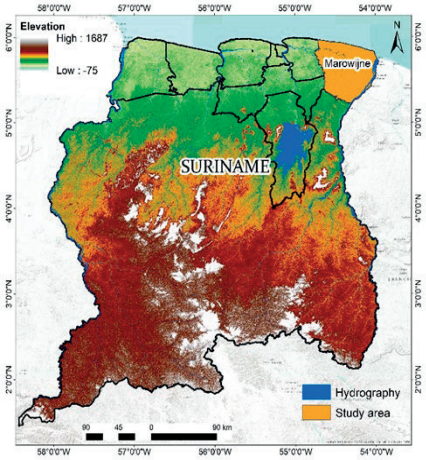

Figure1. Location of the study area

Table 1. Characteristics of data collected

Data	Source	Acquisition year	Scale/ Resolution
Multispectral satellite imagery	Esri Land Cover: https://livingatlas.arcgis.com/ladcover/	2017 2020	10 m
	Google Earth Engine Data Catalogue: https://developers.google.com/earth-engine/datasets/catalog/	2024	
Digital Elevation Model (DEM)	30-Meter SRTM Tile Downloader: https://dwtkns.com/srtm30m/	2018	1-arcsecond (3601x 3601 pixels)
Shape-file with locations of gold mining activity	National Environmental Authority: https://nimos.org/en/about-us/	2018	–
Shapefile with locations of deforestation areas	National Land Monitoring System of Suriname GONINI https://www.gonini.org/	2023	–

Slope, distance from water bodies (rivers and creeks), distance from roads, distance from gold mining and deforestation areas, distance from key settlements (growth poles), and population density datasets were developed individually in 2024 with a spatial resolution of 10 m. These datasets were processed in QGIS 3.34 and ArcGIS 10.8. The Euclidean distance function was employed to generate distance maps from roads, rivers, gold mining areas, and growth poles using vector data of the features (Kafy et al., 2021; Gharaibeh et al., 2020). The DEM was processed in ArcGIS Spatial Analyst tools to create elevation and slope maps.

Image classification. Sentinel imageries for the year 2024 were classified using the Random Forest (RF) classifier and Google Earth Engine (GEE) capabilities.

Random Forest is a non-parametric, multivariate technique known for its ability to handle high-dimensional data and multicollinearity effectively. It is also robust against overfitting and tolerant of suboptimal training data quality (Hemmerling et al., 2021).To evaluate classification accuracy, a random sample comprising 30% of the reference data for 2024 was used. The error matrix, generated in Google Earth Engine (GEE), included key metrics such as overall accuracy and the kappa coefficient (Congalton & Green, 1999; Lu & Weng, 2007). These metrics are widely recognized for measuring the agreement between the classification results and the validation dataset (Mhanna et al., 2023).

The bands 4–3–2 combination (true colour combination), bands 8–4–3 combination (false colour combination) and bands 12–11–4 combination were utilised to perform Sentinel-2 image classification.

A total of 5000 LULC reference data points representing various land use categories, including water, forest-covered and flooded areas, agricultural land, bare ground, built-up areas, and rangelands, were collected within the Marowijne district (Table 2).

Table 2. Major land use land cover types used and their descriptions

LULC class	Class description
Water bodies	Areas covered by rivers, streams, canals and reservoirs
Forest covered area	Landcover with primary trees, palm, and bamboo with a minimum crown tree cover of 30% with the potential to reach a canopy height of a minimum of 5 m and a minimum area of 1.0 hectares
Flooded area	Areas of any type of vegetation with obvious intermixing of water throughout a majority of the year; seasonally flooded area that is a mix of grass/shrub/trees/bare ground
Agricultural land	Includes areas used for perennial and annual crop production, irrigated areas, commercial farms
Bare ground	Includes land areas of exposed soil, bare soil and open areas consisting of sand, rocks and loam
Built-up area	Includes commercial areas, urban, residential, and rural settlements, industrial areas
Rangeland	Open areas covered in homogenous grasses with little to no taller vegetation; wild grasses with no obvious human plotting (i.e., not a plotted field)

Adopted from Karra et al., 2021. Retrieved from https://www.arcgis.com/

This data was derived from field surveys, expert knowledge, and high-resolution imagery from Google Earth Pro (https://earth.google.com/web). The dataset was then randomly split into two groups: 70% for training and 30% for validation (Aryal et al., 2023; Amindin et al., 2024). The training data were used to perform supervised classification, while the validation data were used to evaluate the accuracy of the resulting map (Sawant et al. 2023).

The classification performance was assessed by calculating key metrics, including overall accuracy, user accuracy, producer accuracy, and the kappa coefficient, based on the confusion matrix. The overall accuracy and kappa coefficient for the classified LULC map of 2024 were 90% and 84%. This indicates a reliable and accurate classification of image for analysing land use/land cover change. Figure 2 shows the statistical distribution of LULC classes for 2017, 2020, and 2024 within the area of interest.

Driving variables. Driving variables, also known as driving factors or drivers, represent various biophysical, socioeconomic, and infrastructural elements that influence land use patterns and the processes of land transformation over time.

Recognizing the need to incorporate the potential influence of independent variables in simulating LULC changes (Gharaibeh et al., 2020), this study considered eight key driving variables (Figures 3 to 6).

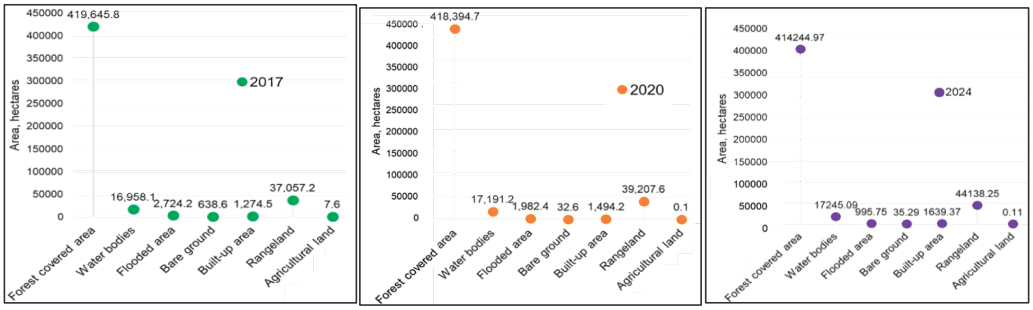

Figure 2. Area of LULC classes in Marowijne district for the years 2017, 2020, and 2024

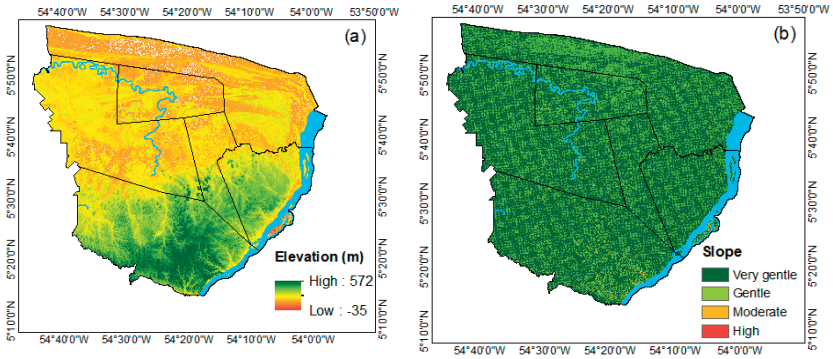

Figure 3. Biophysical driving variables: elevation (a) and slope (b)

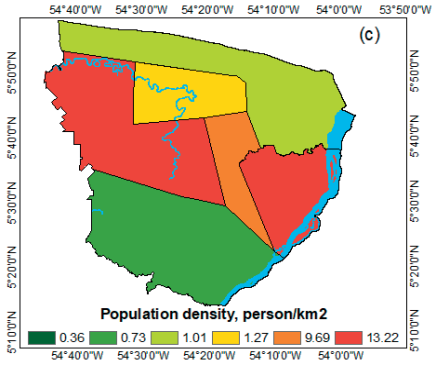

Figure 4. Socioeconomic driving variables: population density (c)

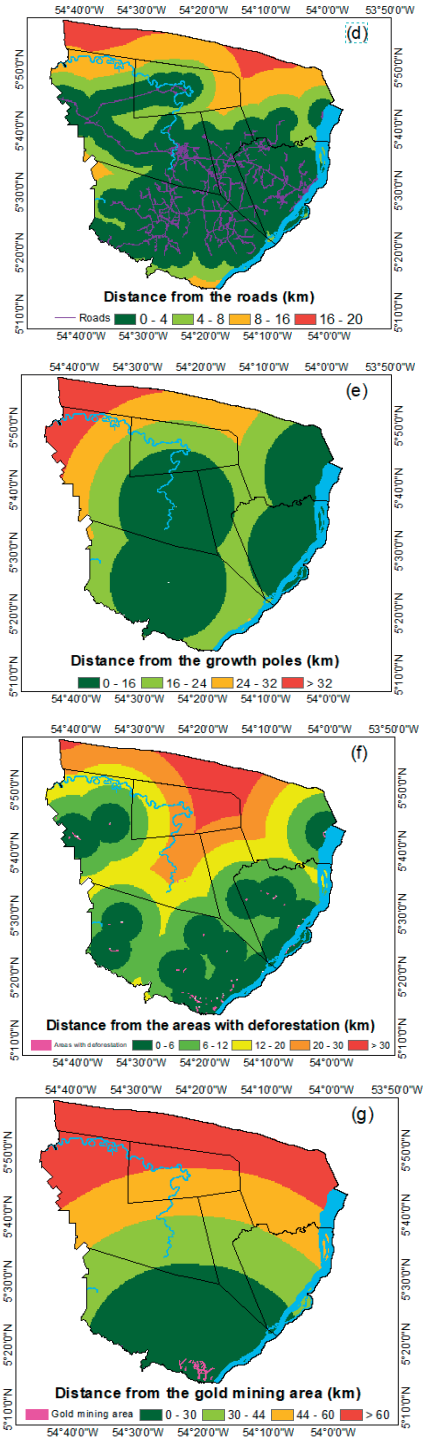

Figure 5. Proximity driving variables: distance from roads (d), growth poles (e), areas with deforestation (f) and gold mining area (g)

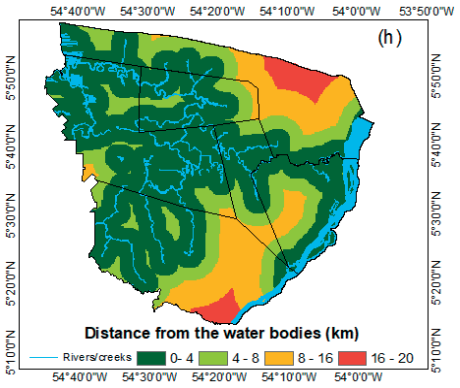

Figure 6. Proximity to water bodies (h)

InVEST model. The InVEST carbon pools model was used to calculate carbon storage and sequestrate potential of landscapes. The carbon storage module of the InVEST model assesses carbon storage using land use types as the units of measurement for the land surface. It can effectively evaluate the quantity and value of ecosystem services. The total carbon storage in the study area was estimated by multiplying the total area of different land types by their corresponding average carbon densities.

The InVEST model was utilized to analyze carbon storage and predict its spatial distribution based on simulated LULC in the area by 2034. The equations are as follows:

$$Ci = Ci_{above} + Ci_{below} + Ci_{soil} + Ci_{dead} \quad (1)$$

$$C_{total} = \sum_{i=1}^{n} Ci \times Si \quad (2)$$

where:

- i is the i-th land use type;
- Ci is the total carbon density of land use type i (Mg·hm^{-2});
- Ci_{above}, Ci_{below}, Ci_{soil} and Ci_{dead} are the aboveground, underground, soil, and dead organic average carbon density of land use type i (Mg·hm^{-2}), respectively;
- C_{total} is the total carbon storage (Mg); Si is the area of land use type i (hm^2);
- n is the number of land use types, with a value of 7 in this study (Maanan et al., 2019; Natural Capital Project, 2023; Li et al., 2023).

The carbon density values of the four carbon pools corresponding to different land use types are shown in Table 3.

YASSO Model. Due to the lack of local data about soil organic matter content the YASSO model (Yasso20) was utilized to assess the soil carbon pool within the study area. This model is a dynamic soil carbon model used to simulate carbon dynamics both in litter and soil organic matter.

Table 3. Biophysical data used in the InVEST carbon storage and sequestration model (unit: Mg/hm^2)

LULC class name	Above ground carbon pool	Below ground carbon pool	Soil carbon pool	Dead wood carbon pool	Data sources
Forest cover	155.34	35.91	27.5*	4.54	Eggleston et al., 2006; SBB; CELOS; CATIE; NZCS, 2017
Flooded area	44.41	10.66	26.55	2.9	
Rangeland	72.63	8.96	26.55	1.94	
Water bodies	0	0	0	0	CELOS; CATIE; NZCS, 2017; Zhang et al., 2019
Bare ground	0	0	0	0	
Built-up area	4.11	0.98	13.5	1.94	
Agricultural land	4.11	0.98	13.5	1.94	Dida et al., 2021; Natural Capital Project, 2023

* – value was estimated with YASSO model.

It predicts the decomposition of organic materials (like plant litter) and the resulting carbon storage and release over time. The model uses climate data (temperature and precipitation) and litter input data to estimate carbon fluxes and long-term soil carbon storage (Viskari et al., 2022).

LULC change detection and simulation. The Land Change Modeler (LCM) within the TerrSet software was applied to analyze and project future LULC changes in the study area. This data-driven, step-by-step approach included change detection, modelling transition potentials, and forecasting changes based on historical data from 2017 to 2020. A Markov probability matrix was employed to estimate the likelihood of transitions between LULC classes over time. Transition potential maps, representing the probability of land use transitions, were generated using a multi-layer perceptron neural network (MLP), support vector machine (SVM), cellular automata (CA), and logistic regression (LR).

Validation of model outputs. The validation process was conducted using the Validate module in the TerrSet software. This module calculated kappa statistics to assess the agreement between the hard prediction and reference map. The computed metrics included kappa for no information (K_{no}), kappa for grid cell-level location ($K_{location}$), kappa for stratum-level location ($K_{locationStrata}$), and kappa standard ($K_{standard}$) (Girma et al., 2022; Mishra et al., 2018). Generally, a strong and acceptable kappa value is considered to be around 80% or higher (Girma et al., 2022; Gharaibeh et al., 2020). For forecasting, the LULC maps from 2017 and 2020 were used as input variables to predict the 2034 LULC distribution. The LULC maps from 2024 and 2034 were utilized as input variables for the InVEST model to predict the 2034 carbon storage and sequestration. Figure 7 illustrates the modelling and validation processes employed in this study.

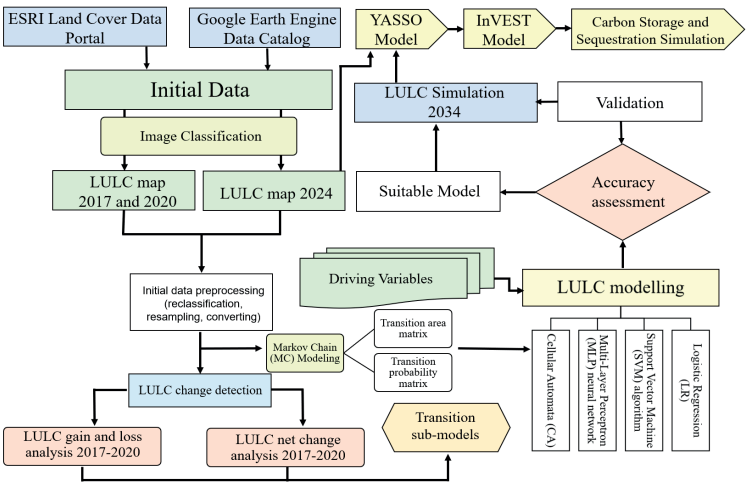

Figure 7. Research design flowchart

RESULTS AND DISCUSSIONS

To accurately predict future LULC trends over the next 10 years, it is pivotal to identify and comprehend past trends in land use and land cover changes (Girma et al., 2022; Regasa et al., 2021). The study area underwent notable landscape transformations and shifts in land use between 2017 and 2020, as shown in Figures 8 and 9.

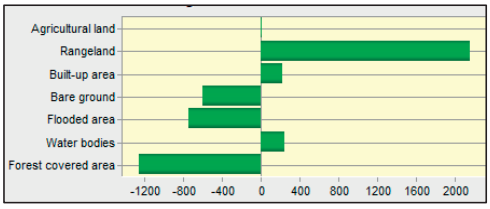

Figure 8. Net changes in LULC within the limits of Marowijne district between 2017 and 2020, hectares

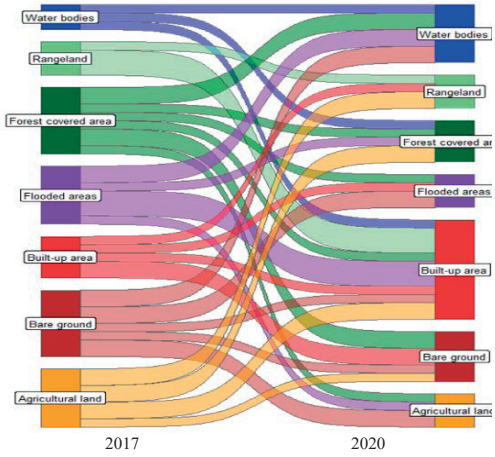

Figure 9. Sankey diagram of LULC classes mutual conversion from 2017 to 2020

A significant conversion of forest-covered areas into rangeland indicates ongoing forest loss, which may negatively impact biodiversity and carbon storage. Considering that over 86% of the district's territory is forested, logging and land clearing for commercial or subsistence farming have been the primary drivers of deforestation from 2017 to 2020.

A decrease in flooded areas suggests the drying or degradation of wetlands, which adversely affects water resources and ecosystem services. These changes are driven by altered hydrological cycles due to climate change, poor water management, and deforestation. The notable net increase in rangeland is primarily attributed to the reduction in forest cover and bare ground. Although built-up areas constitute only 0.3% of the total land in the Marowijne district, they have expanded significantly during the observed period, signaling the intensification of urbanization, particularly within established urban growth poles. The net change in water bodies is mainly influenced by shifts in forest cover and bare ground. The outcomes of the LULC change analysis serve as the foundation for constructing transition sub-models (Table 4). Based on these results, considering the most significant gains and losses for each land use class, seven sub-transition models were identified, the best of which was incorporated into the final predictive model.

This study employed biophysical, socioeconomic, and proximity-related driving variables to predict LULC changes. Before incorporating these drivers into the predictive model, their explanatory power was evaluated. Cramer's V was used to assess the strength of association, while p-values were applied to determine statistical significance (Table 5).

Table 4. Transition sub-models and their descriptors

Transition sub-model	Land cover transition	Description
Forest covered areas losses (FLO)	Forest-covered areas to rangeland, water bodies and built-up area	FLO sub-model describes the process of deforestation where forest areas are replaced by other land-use types such as rangeland, water bodies, or urban development
Forest covered areas gains (FGA)	Bare ground and flooded areas to forest covered areas	Represents reforestation or afforestation where non-forested areas like bare ground or flooded areas are transformed into forest-covered areas
Water bodies transformation (WAT)	Forest-covered areas, flooded areas, bare ground, built-up area and rangeland to water bodies	This refers to the conversion of land types such as forests, flooded areas, bare ground, rangeland, and urban areas into water bodies, often due to flooding or human interventions like dam creation

Transition sub-model	**Land cover transition**	**Description**
Flooded areas transformation (FAT)	Flooded areas to forest covered areas, rangeland and water bodies	Involves the draining or reclamation of flooded areas for conversion into forest, rangeland, possibly for agriculture or urban development
Bare ground transformation (BAT)	Bare ground to forest covered areas, flooded areas, water bodies, built-up areas and rangeland	Bare land transitions into various types, including forest cover, urban areas, or agricultural rangelands, driven by natural ecological succession or deliberate land-use planning
Urban expansion (UEX)	Forest-covered areas, flooded areas, bare ground and rangeland to built-up areas	Describes urban expansion, where natural landscapes like forests and rangelands are converted into residential, industrial, or commercial areas to meet the demands of a growing population within the key settlements
Rangeland transformation (RAT)	Rangeland to forest covered areas, flooded areas and bare ground	Involves the transformation of rangelands into forests or bare land, often resulting from land reclamation initiatives, degradation processes, or targeted reforestation efforts.

Table 5. Cramer's V and p-value for each of the explanatory variables

Driver variables	Cramer's V	p-value
Distance from deforestation	0.2363	<0.0001
Slope	0.2847	<0.0001
Elevation	0.3888	<0.0001
Distance from water bodies	0.3705	<0.0001
Distance from roads	0.3779	<0.0001
Distance from growth poles	0.4012	<0.0001
Distance from gold mining area	0.4026	<0.0001
Population density	0.4600	<0.0001

According to Eastman (2016), Cramer's V values above 0.15 are considered "useful," and values over 0.4 are seen as "good." In this study, population density stands out with the highest Cramer's V of 0.4600, making it the most important factor in explaining changes in land use. The distance from gold mining areas (0.4026) and from growth poles (0.4012) also show strong connections, suggesting that mining and urbanization play major roles in shaping land-use patterns. The proximity to roads (0.3779) and water bodies (0.3705) are somewhat important, reflecting how accessibility and water resources influence land changes. Elevation (0.3888) and slope (0.2847) show a moderate to strong link, emphasizing the role of terrain features in determining land use. While distance from areas of deforestation (0.2363) has the weakest association, it is still statistically significant. All variables are found to be significant predictors of land-use change (p-value <0.0001), with population density, proximity to gold mining, and growth poles having the strongest associations. On the other hand, elevation and slope appear to have the least impact. This analysis underscores the significant role of human-driven factors in land-use changes within the Marowijne district.

To find the most suitable transition sub-model, accuracy rates were calculated for each hybrid model and its respective sub-models. The performance of the LR-MC hybrid model was assessed using the ROC method (Myslyva et al., 2023). A summary of the accuracy assessment for various transition sub-models is provided in Table 6.

Table 6: Hybrid modelling approaches and their accuracy

Transition sub-model	Modelling approach accuracy rate (%)		
	MLP-MC	SVM-MC	LR-MC
FLO	78.95	85.33	72.50
FGA	81.34	91.49	75.20
WAT	64.63	71.50	59.80
FAT	63.97	78.36	57.45
BAT	69.77	73.64	65.30
UEX	92.66	97.14	87.50
RAT	79.45	88.66	73.80

The suitability assessment for various transition sub-models was not conducted for the CA-MC predictive model, as it relied on a transition areas file generated through Markov Chain analysis, which accounted for all-to-all transitions. However, due to the limited availability of historical data on LULC dynamics (covering the period from 2017 to 2020), this model was still selected to predict LULC changes. A model accuracy of 80% or higher is generally considered acceptable to validate training results (Gharaibeh et al., 2020; Silva et al., 2020). As a result, only the LR-MC hybrid model with the UEX transition sub-model, the MLP-MC hybrid models with the FGA and UEX transition sub-models, and the SVM-MC hybrid models with the FLO, RAT, FGA, and UEX transition sub-models met the suitability criteria for LULC

change prediction. However, the overall agreement between the actual LULC map and the CA-MC model-simulated map did not reach the satisfactory range. While previous studies report higher accuracy rates for MLP (Girma et al., 2022; Leta et al., 2021; Gharaibeh et al., 2020; Gibson et al., 2018), this study demonstrated that SVM is a more effective machine learning approach, offering a robust and flexible solution for LULC change prediction. SVM excels at handling complex, non-linear relationships between land cover and its driving factors, resulting in high accuracy. The superior performance of SVM can also be attributed to its ability to work effectively with smaller datasets (Myslyva et al., 2024), such as the limited four-year dataset used in this study. This higher accuracy is reflected in the SVM-MC model, as shown by the parameters in Table 7.

Table 7. Model parameters and accuracy

Parameter	Value
Modelling approach	SVM learning algorithm
Sub-model	Urban expansion (UEX)
Kernel type	Radial Basis Function
Epsilon (ε)	0.0100
Class number	8
Total cross-validation number	272
Total sample number	2272
Overall cross-validation accuracy	0.9714
Overall out-of-sample accuracy	0.9751
Overall skill measure	0.9503

To validate the model, the Kappa statistic (k- index) for quantity and location was computed by comparing the hard simulation with the reference map of 2024 (Table 8).

Table 8. The k-index values of the simulated LULC map of 2024

Index	Value
K_{no}	0.9824
$K_{location}$	0.9848
$K_{locationStrata}$	0.9848
$K_{standard}$	0.9723

The statistics reveal that all kappa index values surpass the satisfactory range (≥ 80%). The overall disagreement between the reference and predictive maps is generally low, primarily attributed to allocation errors (0.0083) rather than quantity errors (0.0071). Despite the presence of allocation errors, the overall agreement between the actual and simulated maps is high, reaching 98.47%.

The developed model was then used to predict future land use changes during next 10 years under the business-as-usual scenario. Figure 10 illustrates the LULC predictive map for the year 2034 and Figures 11 and 12 depicts the transformations in LULC classes between 2024 and 2034.

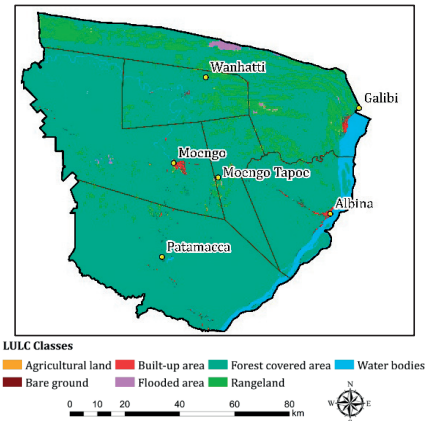

Figure 10. Projected LULC map for the territory of the Marowijne district for 2034

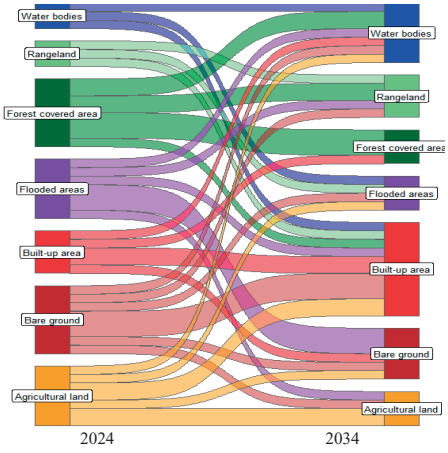

Figure 11. Sankey diagram of LULC classes mutual conversion from 2024 to 2034

The prediction of LULC changes over the next decade offers key insights into how carbon storage and sequestration might be impacted within the area of interest. Between 2024 and 2034, forest-covered areas, essential for storing carbon, are expected to increase slightly by 3,332.39 ha, which could contribute modestly to carbon sequestration. On the other hand, the

significant decrease in rangeland (about 5300 ha) could reduce its ability to act as a carbon sink, especially if these areas are converted to built-up spaces.

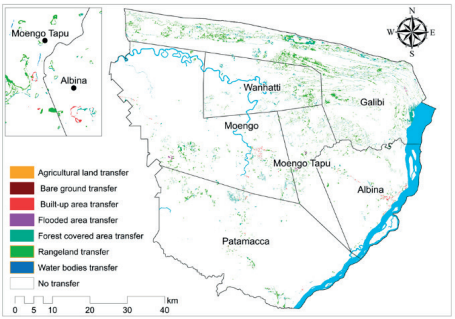

Figure 12. Areas where land use types will change from 2024 to 2034

Urbanization, with built-up areas expanding by about of 1000 ha, will likely lower the carbon sequestration potential as vegetation gives way to impervious surfaces. The rise in flooded areas (also about 1000 ha) could also affect carbon dynamics, as wetlands can either store carbon or release methane, depending on the type of flooding and vegetation. The small reduction in bare ground (-4.64 ha) and minimal changes in agricultural land and water bodies are unlikely to significantly impact carbon storage. Overall, these shifts highlight the complex relationships between land use changes and carbon balance.

The modelling results revealed the spatial and temporal dynamics of carbon storage and sequestration in the Marowijne district from 2017 to 2034 (Figures 13 and 14).

In 2017, areas with high carbon storage (1.8–2.23 MgC/pixel) made up around 40–50% of the district, while those with moderate storage (1.35-1.79 MgC/pixel) covered about 30–40%. Low-storage areas were relatively rare. By 2024, the high-carbon storage areas had decreased to roughly 30-35%, and the moderate storage areas expanded to 40-50%. At the same time, low-carbon storage areas (0.46-0.89 MgC/pixel) will began to spread, covering around 15-20% of the district. Looking ahead to 2034, the high-carbon storage areas are expected to shrink further to 20-25%, while both low and moderate storage areas will likely cover about 25-30% and 50-55%, respectively.

Between 2017 and 2024, reductions in carbon storage affected about 20-25% of the district, primarily in coastal zones and areas around Albina and Moengo. Increases in carbon storage were limited to less than 5%, reflecting localized improvements likely due to afforestation. During the subsequent decade (2024–2034), reductions in carbon storage are expected to intensify and spread to broader areas, particularly in central and coastal zones, affecting 15-20% of the district and focusing on already degraded areas. Only a few areas (under 3%) are projected to exhibit increases, further highlighting a net decline in carbon sequestration potential within the limits of the study area.

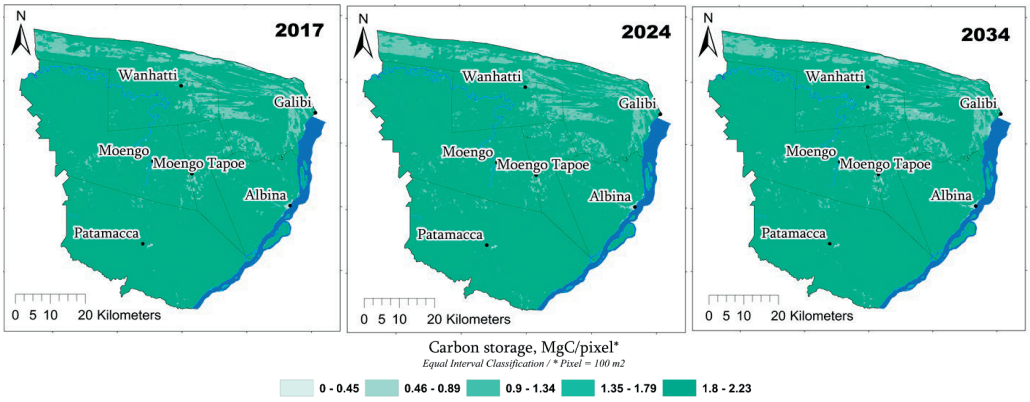

Figure 13. Dynamic of carbon storage and sequestration in Marowijne district

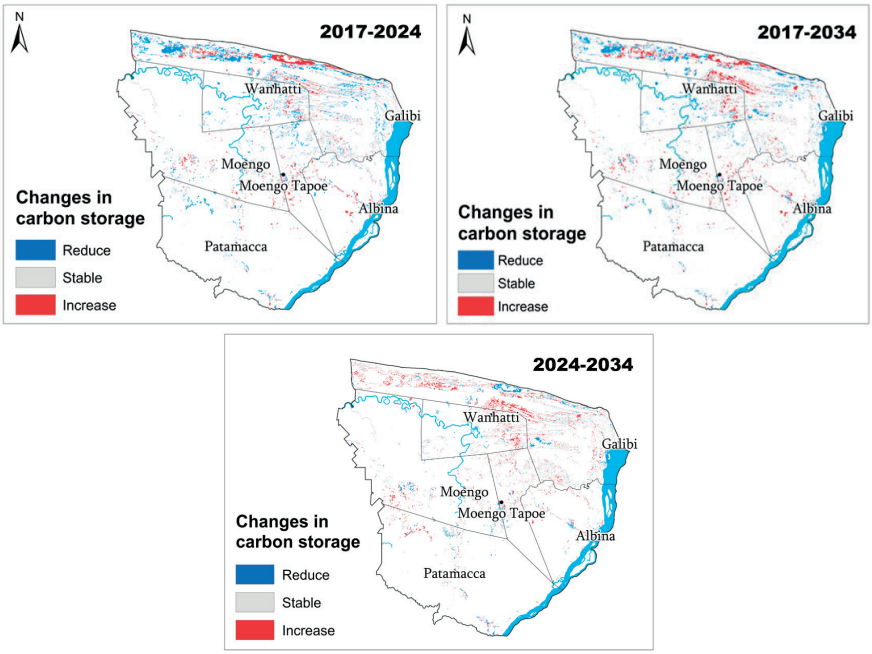

Figure 14. Change areas of carbon storage and sequestration in Marowijne district

Coastal and settlement areas, such as Albina and Moengo, are expected to experience the most significant losses in carbon storage, with reductions impacting 30–35% of the district by 2034. The net loss of high-carbon areas (~15–25%) between 2017 and 2034 reflects intensifying anthropogenic pressures and underscores the urgent need for effective land-use management strategies.

CONCLUSIONS

The transformation of land use and land cover (LULC) in the Marowijne district of Suriname from 2024 to 2034 was simulated using four hybrid predictive models: Markov chain analysis with cellular automata (CA-MC), multilayer perceptron (MLP-MC), support vector machines (SVM-MC), and logistic regression (LR-MC). This research utilized a combination of dependent (driver) and independent spatial datasets, analyzed through both statistical and graphical methods. Eight biophysical, socioeconomic, and proximity variables were identified as the primary drivers of LULC change. Based on the land use change analysis and the most significant gains and losses for each land use class, seven sub-transition models were developed. Among these, the urban-expansion model was selected as the most appropriate for inclusion in the final predictive model.

Accuracy assessments revealed that the SVM-based model, which incorporated the UEX transition sub-model for transitions such as the conversion of forest-covered areas, flooded areas, bare ground, and rangeland to built-up areas, achieved an overall accuracy of 97.14%. While previous studies indicated higher accuracy for MLP models, the SVM model proved superior in this study due to its robustness with small datasets and its ability to effectively handle high-dimensional data. The reliability of the SVM model was further confirmed by a Kappa statistic of 98.47% for predictions in 2024.

Using the business-as-usual scenario, future LULC changes for 2034 were forecasted. The model predicts a slight increase in forest-covered areas, a significant reduction in rangelands, expansion of built-up areas, and an increase in flooded areas. These trends underscore the intricate interplay between human activities and environmental factors,

highlighting the urgent need for sustainable land management practices.

The expected decline in carbon storage suggests a decrease in carbon sequestration, which could have negative effects on both climate regulation and the overall stability of ecosystems. To counteract this loss, it's crucial to implement strategies like reforestation and more stringent land-use policies.

Given the unique characteristics of different resorts in Marowijne, future research should aim to create more specific predictive models that take into account the particular driving factors of each separate resort. This would improve the accuracy of LULC predictions and support more focused, effective land management practices.

REFERENCES

Aloqaili, H., Alomar, S., Elgazzar, R., & Mahmoud, S. (2021). Assessing land suitability and management strategies through LULC models. *Journal of Land Use Science*, *16*(2), 121-139. 8.

Amindin, A., Siamian, N., Kariminejad, N., Clague, J. J., Reza Pourghasemi, H. (2024). An integrated GEE and machine learning framework for detecting ecological stability under land use/land cover changes. *Global Ecology and Conservation*, *53*, e03010.

Aryal, J., Sitaula, C., Frery, A. C. (2023). Land use and land cover (LULC) performance modeling using machine learning algorithms: a case study of the city of Melbourne, Australia. *Scientific Reports, 13*(1), 13510.

Asif, M., Kazmi, J., Tariq, A., Zhao, N., Guluzade, R., Soufan, W., Almutairi, Kh., El Sabagh, A., & Aslam, M., (2023), Modelling of land use and land cover changes and prediction using CA-Markov and Random Forest, *Geocarto International*, *38*(1).

Congalton, R. G., & Green, K. (1999). Assessing the accuracy of remotely sensed data: Principles and practices. Boca Raton, FL: Lewis Publishers.

Deng, X., Liu, H., Li, W., & Zhou, X. (2020). The role of land use/land cover change in carbon sequestration. *Environmental Research Letters*, *15*(6), 064010.

Devi, A. R., Shimrah, T. (2023). Modelling LULC using Multi-Layer Perceptron Markov change (MLP-MC) and identifying local drivers of LULC in the hilly district of Manipur, India. *Environmental Science and Pollution Research International*, *30*(26), 68450–68466.

Dida, J. J., Tiburan, C., Tsutsumida, N., Saizen, I. (2021). Carbon stock Estimation of Selected Watersheds in Laguna, Philippines Using InVEST. *Philippine Journal of Science*, *150*(2), 501–513.

Eastman, J. R. (2016). TerrSet Manual, Geospatial Monitoring and Modeling System. Clark University, Worcester, USA. Clark University, Worcester, USA.

Eggleston, H. S., Buendia, L., Miwa, K., Ngara, T., Tanabe, K. (2006). *IPCC guidelines for national greenhouse gas inventories*. Institute for Global Environmental Strategies, Hayama, Japan, 2, 48–56.

Gharaibeh, A., Shaamala, A., Obeidat, R., Al-Kofahi, S. (2020). Improving land-use change modelling by integrating ANN with cellular automata-Markov chain model. *Heliyon*, *6*.

Gibson, L., Munch, Z., Palmer, A., Mantel, S. (2018). Future land cover change scenarios in South African grasslands – implications of altered biophysical drivers on land management. *Heliyon*, *4*(7).

Girma, R., Fürst C., Moges A. (2022). Land use land cover change modelling by integrating the artificial neural network with cellular Automata-Markov chain model in Gidabo river basin, main Ethiopian rift. *Environmental Challenges, 6*, 100419.

Global Forest Watch. (n.d.). Suriname. Retrieved January 2, 2025, from https://www.globalforestwatch.org.

Hemmerling, J., Pflugmacher, D., Hostert, P. (2021). Mapping temperate forest tree species using dense Sentinel-2 time series. *Remote Sensing of Environment, 267*, 12743.

Kafy, A.-A., Naim, M. d. N. H., Subramanyam, G., Faisal, A.-A., Ahmed, N. U., al Rakib, A., Kona, M. A., Sattar, G. S. (2021). Cellular Automata approach in dynamic modelling of land cover changes using RapidEye images in Dhaka, Bangladesh. *Environmental Challenges*, *4*, 100084.

Karra, K., Kontgis, C., Statman-Weil, Z., Mazzariello, J. C., Mathis, Brumby, M. S. P. (2021). Global land use / land cover with Sentinel 2 and deep learning. 2021 IEEE International Geoscience and Remote Sensing Symposium IGARSS, Brussels, Belgium, 2021, 4704–4707.

Lambin, E. F., & Meyfroidt, P. (2019). Global land use change, economic globalization, and the looming land scarcity. *Proceedings of the National Academy of Sciences*, *116*(15), 7350-7357.

Leta, M. K., Demissie, T. A., Tränckner, J. (2021). Modelling and prediction of land use land cover change dynamics based on land change modeller (LCM) in Nashe watershed, upper Blue Nile basin, Ethiopia. *Sustainability*, *13*.

Li, P., Chen, J., Li, Y., Wu, W. (2023). Using the InVEST-PLUS model to predict and analyze the pattern of ecosystem carbon storage in Liaoning Province, China. *Remote Sensing*, *15*, 4050.

Lu, D., Weng, Q. (2007). A survey of image classification methods and techniques for improving classification performance. *International Journal of Remote Sensing, 28*(5), 823–870.

Luo, Y., Sun, J., Li, Z., & Hu, X. (2021). Evaluating carbon sequestration potential in different land cover types. *Global Change Biology*, *27*(8), 1647-1660.

Maanan, M., Karim, M., Kacem, H., Soukaina, A., Rueff, H., Snoussi, M., Rhinane, H. (2019). Modelling the potential impacts of land use/cover change on terrestrial carbon stocks in north-west Morocco. *International Journal of Sustainable Development & World Ecology*, *26*.

Mhanna, S., Halloran, L. J. S., Zwahlen, F., Haj Asaad, A., Brunner, Ph. (2023). Using machine learning and remote sensing to track land use/land cover changes

due to armed conflict. *Science of The Total Environment*, 898, 165600.

Mishra, V. N., Rai, P. K., Prasad, R., Punia, M., Nistor, M.–M. (2018). Prediction of spatiotemporal land use/land cover dynamics in rapidly developing Varanasi district of Uttar Pradesh, India, using geospatial approach: a comparison of hybrid models. *Applied Geomatics*, *10*(3), 257–276.

Mohamed, A., Worku, H. (2020). Simulating urban land use and cover dynamics using cellular automata and Markov chain approach in Addis Ababa and the surroundings. *Urban Climate*, *31*, 100545.

Muhammad, R., Zhang, W., Abbas, Z., Guo, F., Gwiazdzinski L. (2021). Spatiotemporal change analysis and prediction of future land use and land cover changes using QGIS MOLUSCE plugin and remote sensing big data: A case study of Linyi, China. *Land*, *11*(3), 419.

Myslyva, T., Dasai, M., Huisden, C. M., Nadtochiy, P., Bilyavskyi, Y. (2024). Application of machine learning approaches for land use change modelling in Suriname. *Scientific Papers. Series E. Land Reclamation, Earth Observation and Surveying, Environmental Engineering, 13*, 830–840.

Myslyva, T., Nadtochiy, P., Bilyavskyi, Y., Trofymenko, P. (2023). Intra-field spatial heterogeneity prediction for the purposes of precision farming: Comparison of frequency ratio and Shannon's entropy models. *Scientific Papers. Series A. Agronomy, 66*(1).

Natural Capital Project. (2023). InVEST (Integrated Valuation of Ecosystem Services and Tradeoffs) Version 3.14.2. Stanford University, University of Minnesota, The Nature Conservancy, and World Wildlife Fund.

Regasa, M. S., Nones, M., Adeba, D. (2021). A review on land use and land cover change in Ethiopian basins. *Land*, *10*(10), 585.

Robinson, D.T., (2021), Towards a spatially explicit agent-based model of land use change and ecosystem service provisioning in semi-arid rural regions. *Environmental Modelling and Software*, *139*, 104990

Sarathchandra, C., Abebe, Y. A., Worthy, F. R., Wijerathne, I. L., Ma, H., Yingfeng, B., Jiayu, G., Chen, H., Yan, Q., Geng, Y., Weragoda, D. S., Li, L.-L., Fengchun, Y., Wickramasinghe, S., & Xu, J. (2021). Impact of land use and land cover changes on carbon storage in rubber-dominated tropical Xishuangbanna, South West China. *Ecosystem Health and Sustainability*, *7*(1), 1915183.

Sawant, S., Garg, R. D., Meshram, V., Mistry, S. (2023). Sen-2 LULC: Land use land cover dataset for deep learning approaches. *Data in Brief*, *51*, 109724.

SBB; CELOS; CATIE; NZCS. 2017. State-of-the-art study: Best estimates for emission factors and carbon stocks for Suriname. SBB. Paramaribo, Suriname.

Silva, L. P. E., Xavier, A. P. C., da Silva, R. M., Santos, C. A. G. (2020). Modeling land cover change based on an artificial neural network for a semiarid river basin in northeastern Brazil. *Global Ecology Conservation*, *21*.

Song, C., Xu, B., Caylor, K. K. (2020). Impact of deforestation and urbanization on ecosystem services. *Ecosystem Services*, *42*, 101114.

van Ommeren-Myslyva, T., Satnarain, U., Wesenhagen, F. (2024). Hybrid modelling approach for land use change prediction and land management in the Coronie district of Suriname. *South Asian Journal of Management Research*, *14*(4), 388–406.

van Ommeren-Myslyva, T., Wesenhagen, F., Kadirbaks R., Abdoelrahman F. (2024). Application of machine learning approaches for land use change modelling in Commewijne district of Suriname. *Science and Innovation*, *3*, 13–29.

Viskari, T., Pusa, J., Fer, I., Repo, A., Vira, J., Liski, J. (2022). Calibrating the soil organic carbon model Yasso20 with multiple datasets. *Geoscientific Model Development*, *15*, 1735–1752.

Yeh, C.-K., Liaw, S.-C. (2021). Applying spatial autocorrelation and logistic regression to analyze land cover change trajectory in a forested watershed. *Terrestrial, Atmospheric and Oceanic Sciences*, *32*, 35–52.

Zhang, Y., Kong, D., Gan, R., Chiew, F. H. S., McVicar, T. R., Zhang, Q., Yang, Y. (2019). Coupled estimation of 500 m and 8-day resolution global evapotranspiration and gross primary production in 2002–2017. *Remote Sensing of Environment*, *222*, 165–182.